

# Report on Robotic swimmer

Kedar Joshi, Pulkit Katdare, Naman Gupta

November 2, 2016

## 1 Introduction

Swimming has received attention in fields ranging from robotics to fluid mechanics to biology. The physics of self-propulsion through a surrounding fluid have long driven new results in these areas and led to insightful observations regarding the behavior of swimming organisms; in robotics these observations serve as guides for the design and control of micro-swimmers and novel aquatic systems. Biological microorganisms swim with flagella and cilia that execute nonreciprocal motions for low Reynolds number (Re) propulsion in viscous fluids. This symmetry requirement is a consequence of Purcell's scallop theorem, which governs the actuation scheme needed by microswimmers. Coming to Purcell's scallop theorem, which deals particularly with low Re states that in this domain inertia plays no role at all. The physics or dynamics of the system are dependent on factors only at that instant of time and nothing before that. As part of our work, we have used Purcell's scallop theorem, dynamical equations derived from Geometric Swimming at Low and High Reynolds numbers by Ross Halton and idea of prototyping the 3-link swimmer from Swimming by reciprocal motion at low Reynolds number by Peer Fischer. The prototype consists of 3-links, two of them driven by servo motor controlled by arduino nano enclosed within the central link/body. It is made waterproof by making use of a special coating over the 3D printed material.

## 2 Purcell's scallop theorem

The ratio of inertial forces to viscous forces is called Reynolds number. At low Reynolds number, inertia plays no role at all. Whatever you are doing at the moment is entirely determined by forces that are exerted on you at that moment and nothing else. Putting a body into low Reynolds number flow constraints the body to deform in some manner. In this regime we study a reciprocal motion, which is to change the form of body and going back to original shape through a sequence in reverse. Time doesn't make any difference, only configuration matters. Changing quickly or slowly, the pattern of motion is exactly the same. The example of scallop is discussed further.

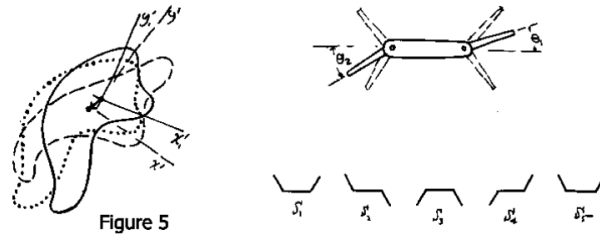


Figure 1: Source: see[2]  
Strokes in a Scallop

We know that a scallop opens its shell slowly and closes its shell fast, squirting out water. The moral of this is that the scallop at low Reynolds number is no good. It can't swim because it only has one hinge, and if you have only one degree of freedom in configuration space, you are bound to make a reciprocal motion. Examples like a torus, two cells stuck together by some kind of attraction here while releasing there or a flexible oar or a corkscrew. Imagine that you are allowed to row a boat in molasses (low Reynolds number). The point is you cannot move because the stiff oars are just reciprocating things. But if the oar were flexible it would break symmetry and hence the scallop theorem will not hold true. Even there is no reciprocal motion with a corkscrew and hence you will be propelled. Coming to real world animals, consider these species as in the figure below. The one we're going to be talking about most is the famous animal, *Escherichia coli*, at A, which is a very tiny thing. Then there are two larger animals. I've copied down their Latin names and they may be old friends to some of you here. This thing (*S. volutans*) swims by waving its body as well as its tail and roughly speaking, a spiral wave runs down that tail. The bacterium *E. coli* on the left is about 2 micron long. The tail is the part that we are interested in. That's the flagellum. Some *E. coli* cells have them coming out the sides; and they may have several, but when they have several they tend to bundle together. Some cells are nonmotile and don't have flagella. They live perfectly well, so swimming is not an absolute necessity for this particular animal, but the one in the figure does swim. The flagellum is only about 130 angstrom in diameter. It is much thinner than the cilium which is another very important kind of propulsive machinery.

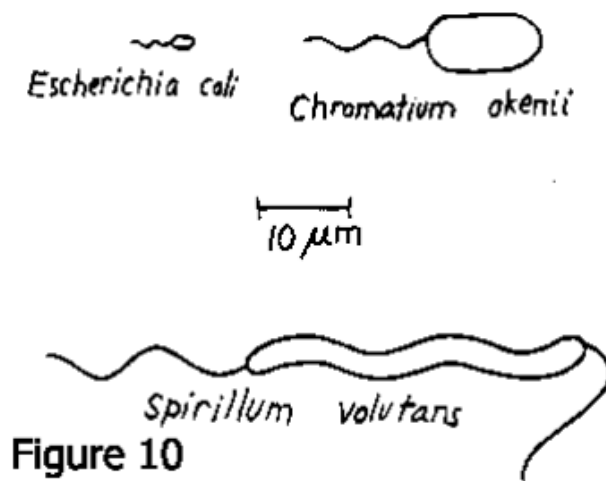


Figure 2: Source: see[2]  
Examples of low Reynolds number organisms

They can rotate hundreds of revolutions at constant speed and then turn around and rotate the other way. Evidently the animal actually has a rotary joint, and has a motor inside that's able to drive a flagellum in one direction or the other, a most remarkable piece of machinery. The point is not how they swim. Turn anything—if it isn't perfectly symmetrical, you'll swim. At low Reynolds number you can't shake off your environment. If you move, you take it along; it only gradually falls behind. Motion at low Reynolds number is very majestic, slow, and regular. You'll notice that the model is actually rotating but rather little. If that were a corkscrew moving through a cork of course, the pattern in projection wouldn't change. It's very very far from that, it's slipping, so that it sinks by several wavelengths while it's turning around once. If the matrix were diagonal, the thing would not rotate at all. So all you have to do is just see how much it turns as it sinks and you have got a handle on the off-diagonal element. A nice way to determine the other elements is to run two of these animals, one of which is a spiral and the other is two spirals, in series, of opposite handedness. The matrices add and with two spirals of opposite handedness, the propulsions matrix must be diagonal (Fig. 14). That's not going to rotate; it better not.

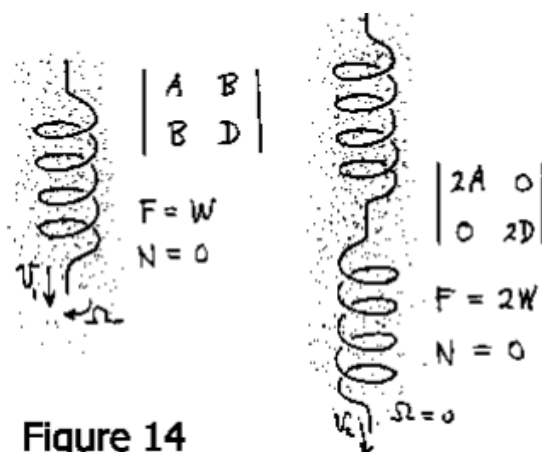


Figure 14

Figure 3: Source: see[2]

An example of stirring vs. diffusion is discussed to show different effects at low reynolds number.

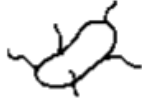
Stirring vs. Diffusion

time for transport by stirring:  $\frac{l}{v}$

time for transport by diffusion:  $\frac{l^2}{D}$

stirring works if  $\frac{lv}{D} > 1$

$S = \frac{lv}{D}$        $\left[ R = \frac{lv}{v} \right]$   
 $< 10^{-5} \text{ cm}^2/\text{sec}$        $< 10^{-2} \text{ cm}^2/\text{sec}$


 $S \approx 10^{-2}$

local stirring accomplishes nothing

**Figure 18**

Figure 4: Source: see[2]

Stirring vs Diffusion

The bug shown above, can't do anything by stirring its local surroundings. It might as well wait for things to diffuse, either in or out. The transport of wastes away from the animal and food to the animal is entirely controlled locally by diffusion. You can thrash around a lot, but the fellow who just sits there quietly waiting for stuff to diffuse will collect just as much. The rule is, to out swim diffusion you have to go a distance which is equal to or greater than this number we had in our  $S$  constant. for typical  $D$  and  $v$ , you have to go about  $30 \mu\text{m}$  and that's just about what the swimming bacteria were doing. If you don't swim that far, you haven't gone anywhere, because it's only on that scale that you could find a difference in your environment with respect to molecules of diffusion constant  $D$ . The crux of this theorem is covered is shown in this figure.

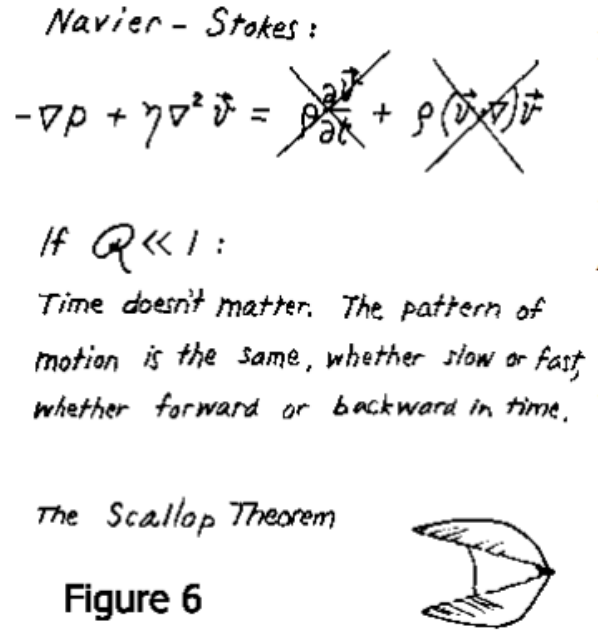


Figure 5: Source: see[2]  
Navier Stokes Approximation

### 3 Control law for 3-link swimmer

Several efforts have recently been made to relate the displacement of swimming three-link systems over strokes to geometric quantities of the strokes. More recently, the strokes themselves have been the focus of attention, with optimal patterns found at low Reynolds number. Whilst these optimizations have primarily been achieved by parameterizing a stroke primitive and then applying standard optimization techniques find the parameters which give the best performance, a second research thrust has applied curvature techniques based on Lie brackets to differential geometric formulations of the system models to directly find useful strokes. These approaches present the net displacement only in terms of rotations and approximations of net translation due to shape change. The paper discusses two important developments, connection vector fields which provides a visual representation of kinematics of locomoting systems and second, optimized coordinate choice. The primary purpose is to demonstrate the applicability of the second tool to swimming systems at high and low Reynolds numbers. The motion of swimmers is dictated by reconstruction equation which encodes the constraint forces and momentum as functions of system shapes and shape velocity. The reconstruction equation simplifies to a kinematic form, generated from drag forces or net conservation of momentum between swimmer and surroundings. The general reconstruction equation is of the form :

$$\xi = -A(r)\dot{r} + \Gamma(r)p \quad (1)$$

Where  $A(r)$  is the local connection, a matrix which relates joints to body velocity,  $\Gamma(r)$  is the momentum distribution coefficient function and  $p$  is gener-

alized non-holonomic momentum, which captures how the system is coasting any given time. The kinematic reconstruction equation looks like as follows,

$$\dot{\xi} = -A(r)\dot{r} \quad (2)$$

At very low Reynolds numbers, viscous drag forces dominate the fluid dynamics of swimming and any inertial effects are immediately damped out. First, the drag forces on the swimmer are linear functions of the body and shape velocities. Second, the net drag forces and moments on an isolated system interacting with the surrounding fluid go to zero: if the swimmer were to move with any velocity other than that dictated by force equilibrium, the large viscous forces would almost instantaneously remove this excess velocity, returning the system to the equilibrium velocity.

## 4 Optimal Strokes

We see that dynamics of our equations are of the form,

$$\dot{\xi} = A(r)\dot{r} \quad (3)$$

We see that the expressions of  $A(r)$  are complicated. One of the ways of visualizing them ( $A(r)$ ) is by making geometrical plots of these local connections. We can visualize each row of  $A(r)$  as defining a vector field on shape space whose dot product with the shape velocity corresponds to corresponding change in body velocity.

$$\dot{\xi}_i = \vec{A}^i(r) \cdot \dot{r} \quad (4)$$

We then geometrically plot each one of them as shown below,

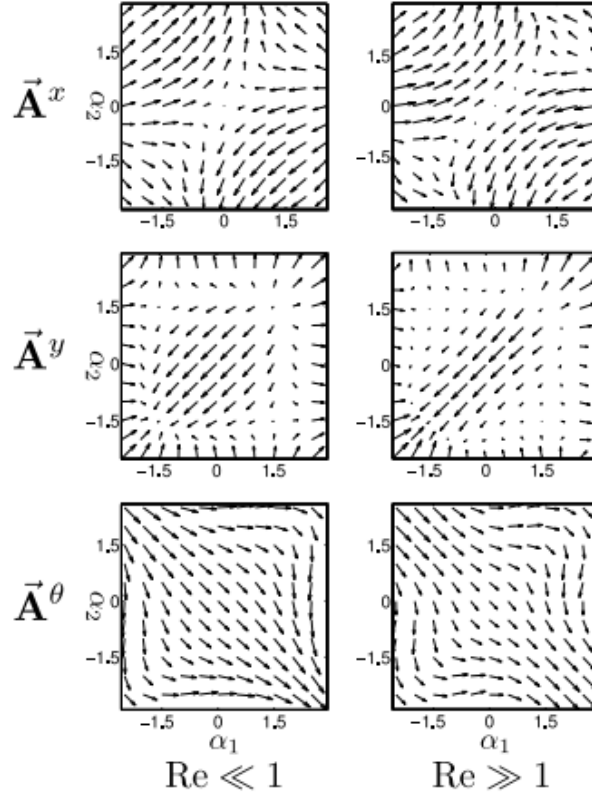


Figure 6: Source: see[1]  
Connection vector fields for low and high Reynolds number

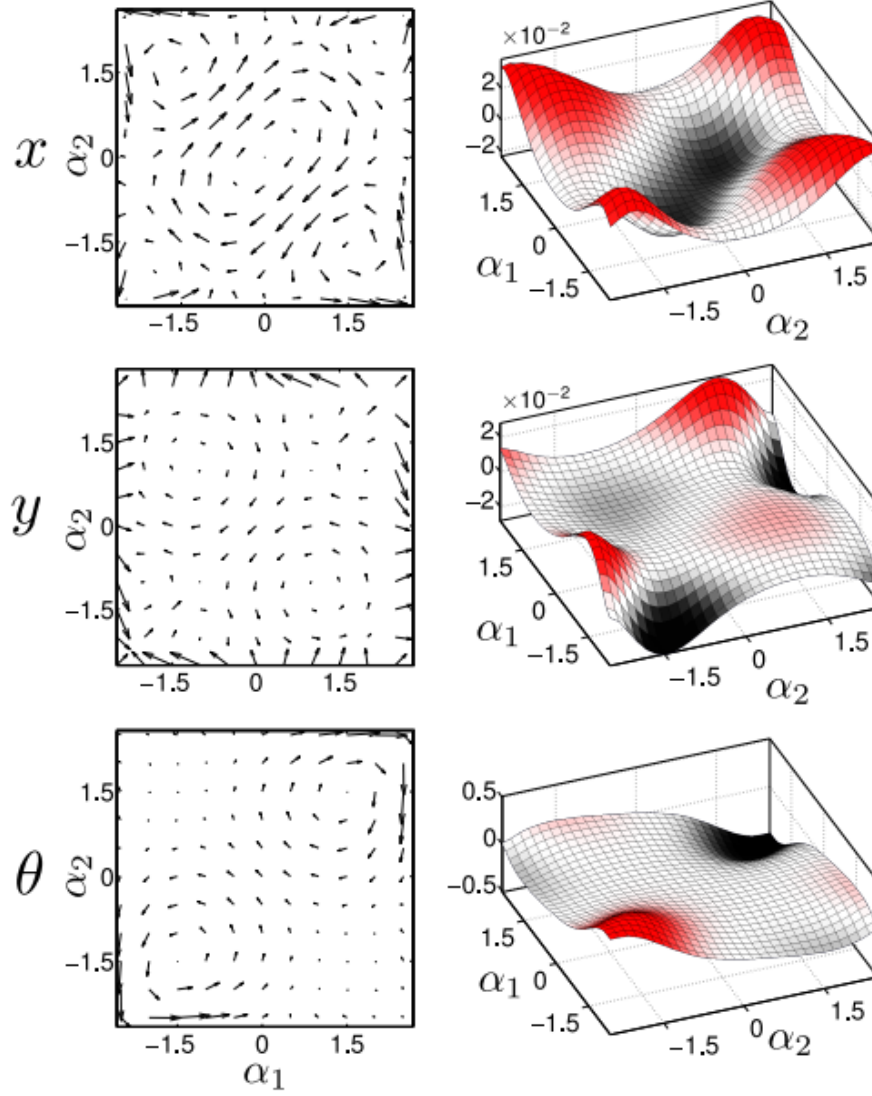
## Constraint Curvature Functions

The problem with geometrical plots as shown above is that it fails to give us information regarding net change in motion over sequence of shape motions. Knowledge regarding such things are very important with respect to controlling their behavior and motion planning. The curvature of local connection is very good at encoding such information in the form of constraint curvature equation(**CCFs**) over shape space. We define the curvature function over a region in shape space bounded by  $\phi$  as follows,

$$z(\phi) = \iint_{\phi} \overbrace{\underbrace{-curl A}_{\text{non-conservativity}} + [A_1, A_2] dr}^{CCFs(fullLieBracket)} + \text{higher-order terms} \quad (5)$$

An interesting property of the curvature equation(5) is that more the stroke amplitude( $\phi$ ) more the intermediate rotations and more the non-commutativity in the displacement(i.e net displacement can't be determined by simple area integration). This has been one of the limitations in determining the admissible stroke size. One of the ways around this to find a new coordinates system(Optimized coordinates) where the non-commutativity in the curvature terms is minimum so that we can qualitatively determine the optimal stroke( $\phi$ ) as the one which encloses maximum area under the CCF curve.

The connection vector fields and the CCFs for optimized coordinates is as shown below,



(a) Low Reynolds number

Figure 7: Source: see[1]

Connection vector fields for low and CCFs for low Reynolds number systems.

## Analysis of Optimality

We see from the  $x$ -CCFs of the coordinates as shown above (figure 7) that the optimal stroke ( $\phi$ ) is the one which covers the maximum area under  $x$ -CCF curve which can be inferred from figure above as the one with 'peanut' shape. (As illustrated below).



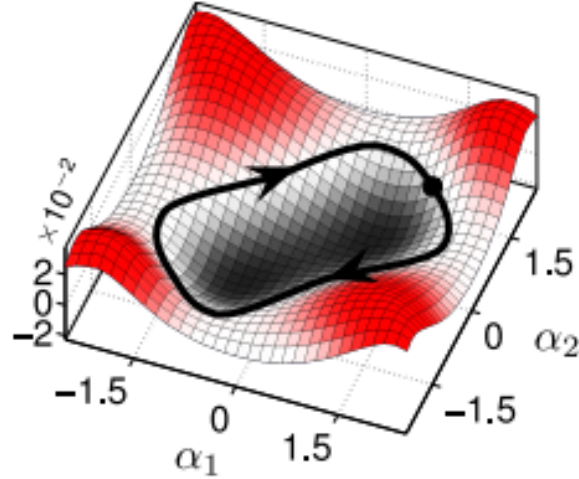


Figure 8: Source: see[1]  
'peanut' shape optimal stroke using CCFs

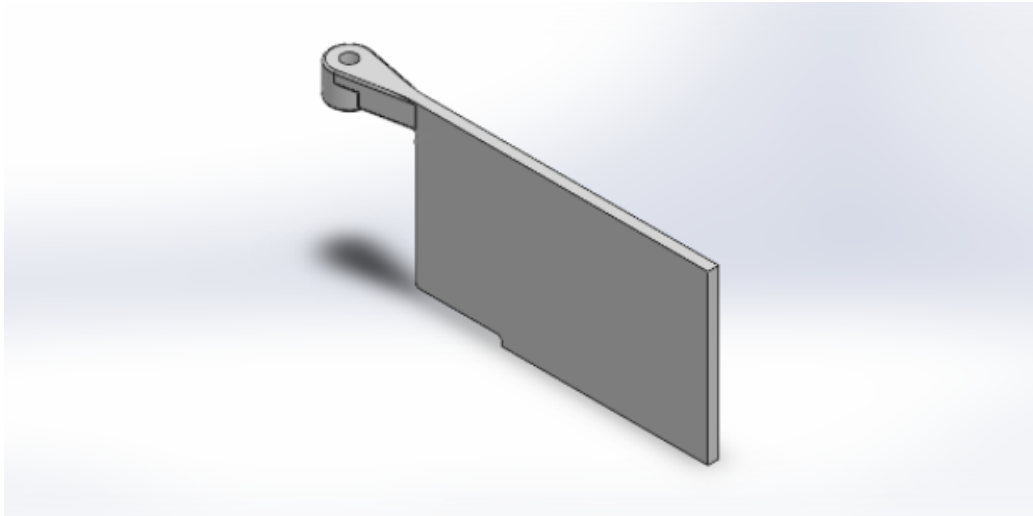
This was also illustrated by Tam and Hanoi(see [3]) while trying to determine the optimal stroke patterns. Their basic finding was that that optimal strokes tend to be rounded oblongs with maximum displacement per cycle pinched at the center. This made them to propose a 'peanut' shape optimal stroke by direct optimization over the space of stroke optimized by fourier series. The reason behind such an optimal stroke can be easily seen by the figure above(figure(8)). Please note that we are looking for optimal strokes that maximise the displacement keeping in view the efficiency of the strokes too. For example to come up with a better optimal stroke we could make a loop that encompasses the corners of the  $x$ -CCFs which produces more displacement per stroke but will lead to a pretty high loss in the efficiency. Hence our search space in this case was to look at simple loops around the origin to maximise our efficiency.

## 5 Prototype of Purcell's 3 link Swimmer

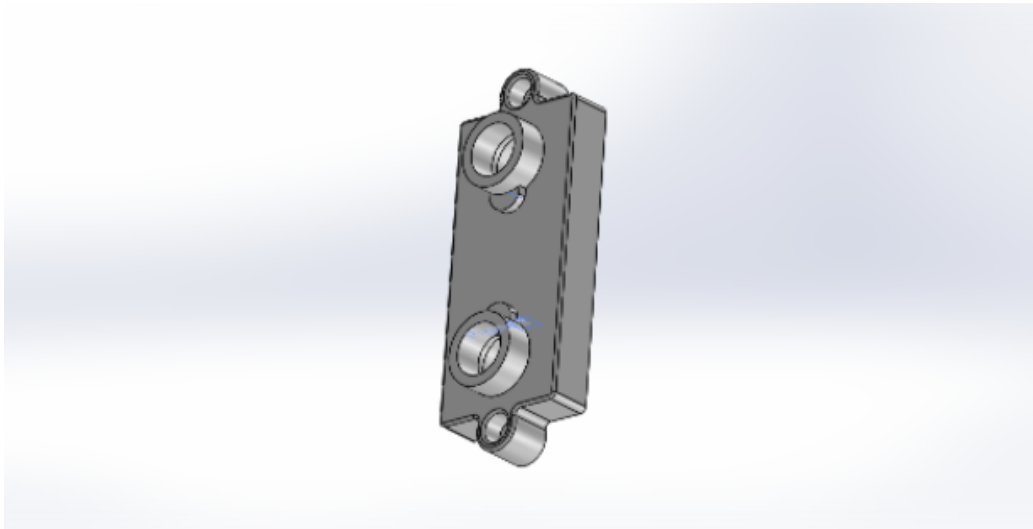
### Parts

**Model:** The model was 3D printed using Nylon/PA 12(White opaque) coated with SLS painting to make it waterproof. The model used 3 links with middle links consisting of three different parts bolted to each other and then sealed using M-seal and rubber tubes.

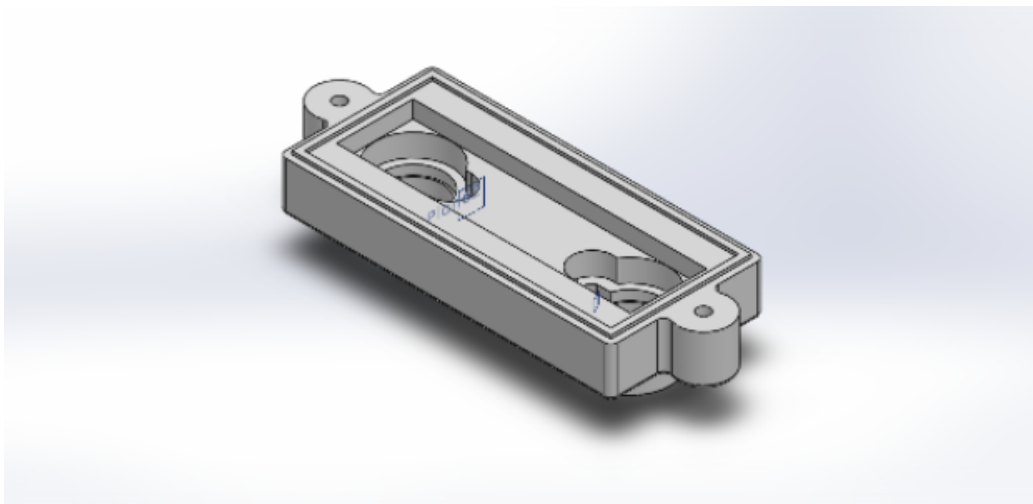
## Moving Link



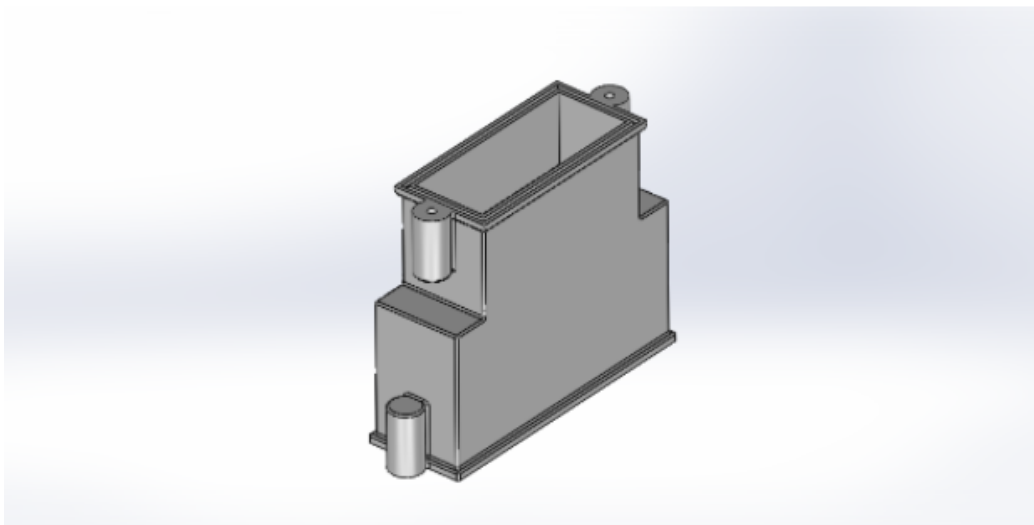
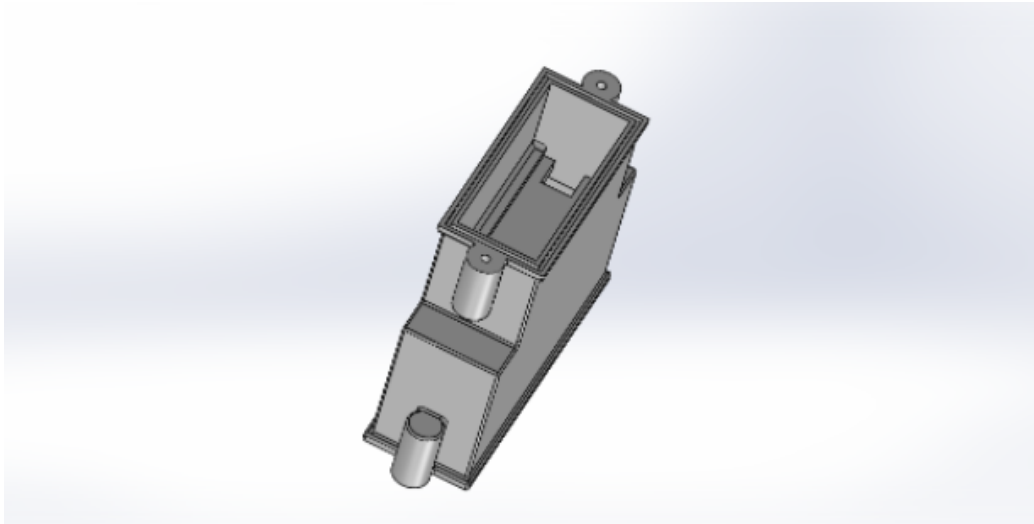
Part for enclosing the servo motors:(Upper view)



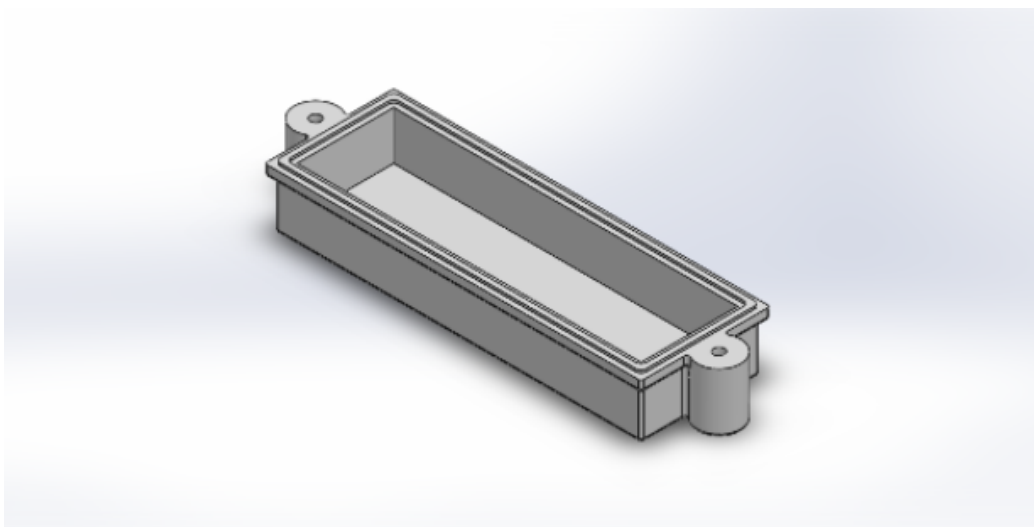
(Bottom view)



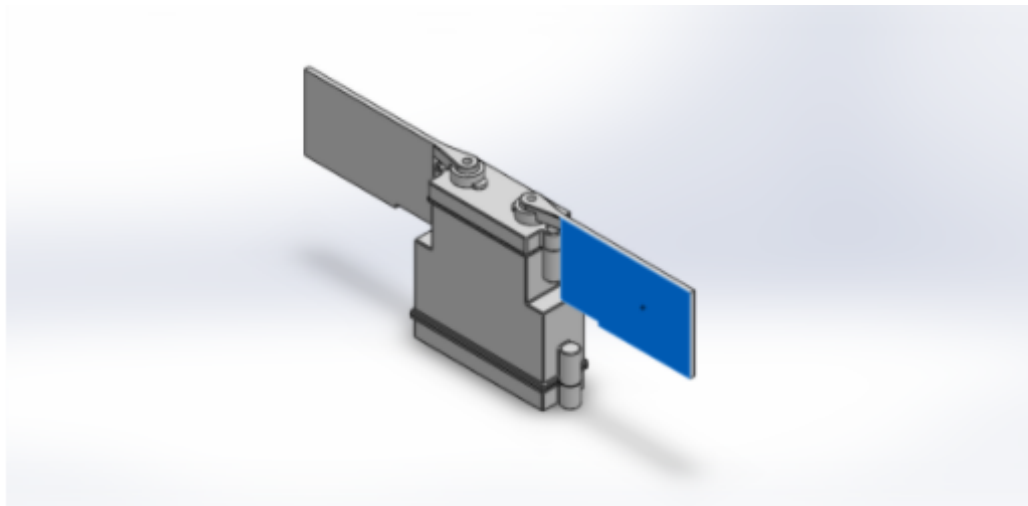
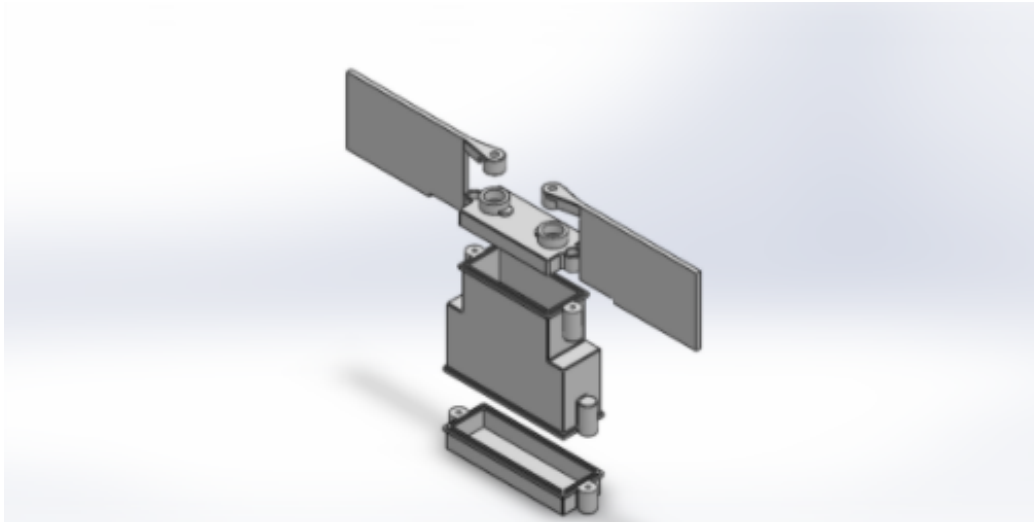
Middle Link which encloses controller, batteries and servo motors



Lid for the middle part:



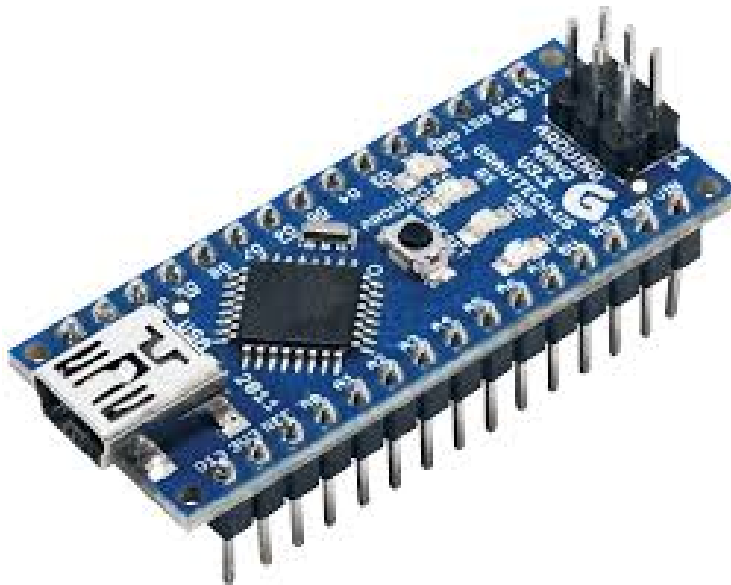
## The Assembly



**Servo Motors:** The servo used were Corona 939-MG, which had 3 wires, two for power and other one for control input. It was waterproof and hence there were no issues with it being within water. The details can be found here ( [https://www.hobbyking.com/en\\_us/corona-939mg-digital-metal-gear-servo-2-7kg-0-13sec-12-5g.html](https://www.hobbyking.com/en_us/corona-939mg-digital-metal-gear-servo-2-7kg-0-13sec-12-5g.html))



**Controllers:** The controller used was Arduino Nano. Specifically because of its small size and better functionality. We had to remove some parts out of the nano board when they became a constraint to fit inside the body (like longer pins). In future we can use which has wifi capabilities so that data can be retrieved wirelessly. For details regarding the power requirements and pin diagram click on the link here(<https://www.arduino.cc/en/Main/ArduinoBoardNano>)

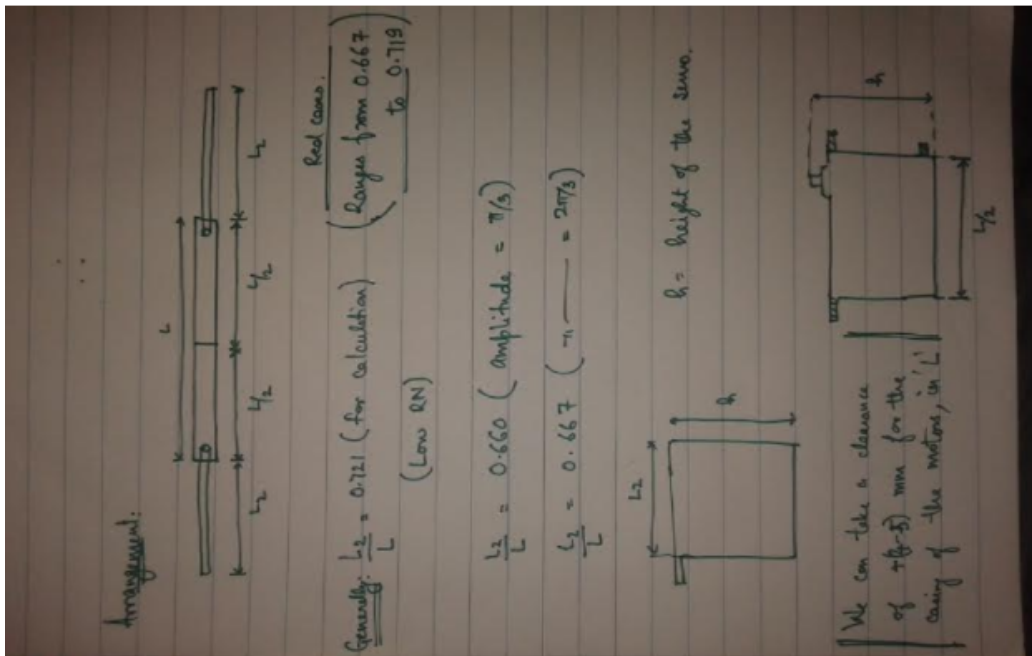


**Batteries:** The specification of the batteries can be found here(<https://www.fabtolab.com/lipo-3.7v-1S?search=Lipo%20Battery%203.7V> )

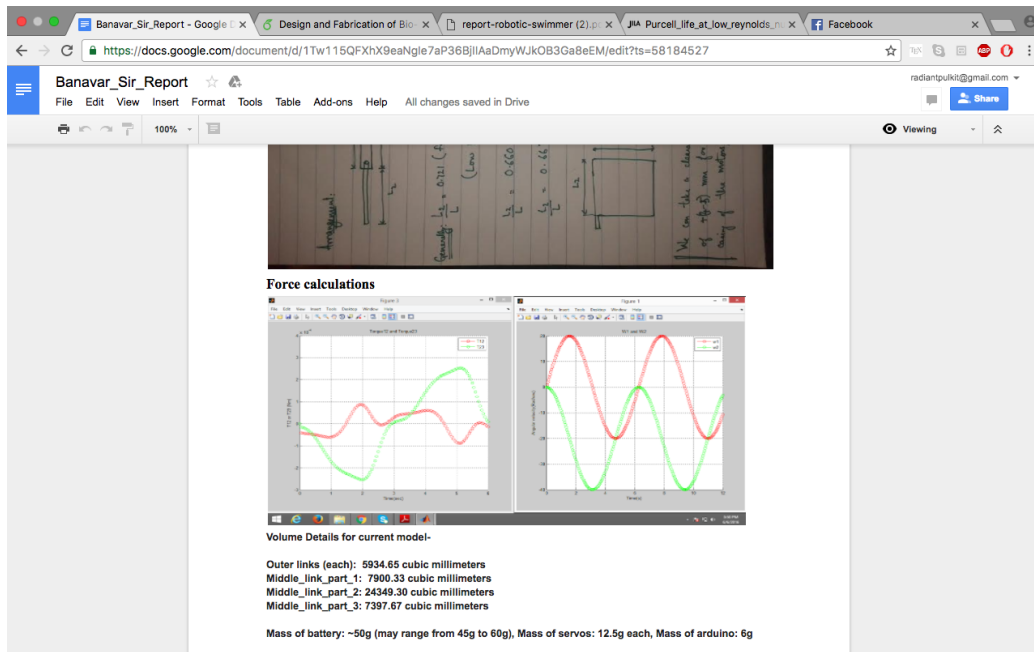


### Calculation for the dimensions

The length  $L/2$  is equal to length  $B$ . And rest of the details are available in the image attached. First Servo:  $L = (84 + 5)$  mm,  $L_2 =$  use the respective ratios to calculate the value,  $h = (41 + 2.5)$  mm First Servo:  $L = (46 + 5)$  mm,  $L_2 =$  use the respective ratios to calculate the value,  $h = (31 + 2.5)$  mm



### Force Calculations



### Volume Details for the current model

Outer links (each): 5934.65 cubic millimeters

Middle\_link\_part-1: 7900.33 cubic millimeters

Middle\_link\_part-2: 24349.30 cubic millimeters

Middle\_link\_part-3: 7397.67 cubic millimeters

Mass of battery: 50g (may range from 45g to 60g), Mass of servos: 12.5g each, Mass of arduino: 6g

## 6 References

1. R.L. Hatton & H. Choset, "Geometric Swimming at Low and High Reynolds Numbers," IEEE Transactions on Robotics, June 2013
2. E. M. Purcell, Life at low Reynolds numbers, American Journal of Physics, vol. 45, no. 1, pp. 311, January 1977.
3. D. Tam and A. E. Hosoi, Optimal stroke patterns for Purcells three-link swimmer, Phys. Review Letters, vol. 98, no. 6, p. 068105, 2007.